Multiple Trapping of Hydrogen in Antimony-Doped Silicon

Z. N. Liang, C. Haas, and L. Niesen

Materials Science Center, Groningen University, Nijenborgh 4, 9747 AG Groningen, The Netherlands

(Received 1 October 1993)

We have employed Mössbauer spectroscopy and low H implantation to study the Sb-H complexes in n-type Si. The different Mössbauer components were studied as a function of H dose, H-implantation temperature, and annealing temperature. To understand the observed data, it is necessary to introduce, in addition to the well-known SbH complex, an SbH_n complex ($n \geq 2$), which provides experimental evidence for the existence of donor-multihydrogen complexes. We show that these complexes are in thermal equilibrium with a larger hydrogen reservoir (H_2^*), which governs their thermal stability.

Introduction of hydrogen in Sb-doped crystalline Si (c-Si) gives rise to passivation, due to the formation of neutral Sb-H complexes [1,2]. Microscopic models have been given for neutral P-H [3] and As-H [4] complexes, which provide vibration frequencies consistent with the experimental results [1]. However, these complexes cannot account for all the H present, because the total H concentration is much higher than the dopant concentrations, as measured by secondary ion mass spectrometry (SIMS) [5-7]. In n-type c-Si, hydrogen forms complexes which have been designated "H_2^*" [7] to distinguish them from the stable and much less mobile "H_2" that forms in p-type Si [6]. A possible microscopic model has been proposed for H_2^* [8,9]. The trapped H appears to scale with the shallow dopant concentration and is present at depths greater than those associated with hydrogen platelets [10,11]. This suggests that multihydrogen complexes form near shallow dopants. Recent *ab initio* Hartree-Fock calculations [12,13] suggest the trapping of a second interstitial H at an already H-passivated P impurity. However, no direct experimental evidence has been obtained thus far for the existence of donor-multi-H complexes in n-type c-Si.

Studying the multiple trapping of H is interesting not only for its own sake, but also for the issue of thermal stability of various H-associated complexes. Zhu, Johnson, and Herring [14] have investigated the P-H dissociation kinetics and obtained an activation energy of 1.18 eV. The activation energy for dissociation for an Sb-H complex falls in the range 1.36-1.46 eV as reported by Bergman *et al.* [1] and Liang and Niesen [15,16]. However, we will show that these results have to be reinterpreted because the coexistence of other H-associated complexes was not carefully considered.

In this Letter, we present studies of Sb- and H-doped silicon using Mössbauer spectroscopy. We have studied in detail the effects of (1) the total H dose, (2) the temperature dependence of the H implantation, and (3) thermal annealing. The data are analyzed in terms of a simple model which describes the kinetics of formation and dissociation of the various hydrogen complexes. To account for the observed data it is necessary to introduce three species in thermal equilibrium: the well-known SbH complex, an additional SbH_2 complex, and a reservoir consisting of H clustered in the form of H_2^*.

Conversion electron Mössbauer spectroscopy (CEMS) [17] has been successfully used for the study of Sb-H complexes in n-type c-Si [15, 16,18]. Before introduction of the hydrogen all ^{119}Sb atoms were at substitutional sites, characterized by a single line with an isomer shift $\delta = 1.80$ mm/s and linewidth of 0.80 mm/s. Introduction of hydrogen results in two phenomena: (1) Another line appears with $\delta = 2.34$ mm/s and linewidth of 0.85 mm/s and (2) the total integrated intensity of the Mössbauer spectrum decreases noticeably. All spectra can be fitted very well with these two lines. Therefore, we decompose the spectrum of the H-implanted sample in three components: the substitutional ^{119}Sb component (I_S), an SbH complex component (I_H), and the "invisible" part given by $I_I = I_0 - I_S - I_H$, where I_0 is the total intensity at the sample temperature (80 K in this case) before hydrogenation [16]. In doing so, we ignore the possible difference in recoilless fraction between the two visible components. This may change the intensities of the various components slightly, but has no consequences for the rest of the discussion. The large reduction of the Mössbauer intensity after hydrogenation must be caused by large displacements of the ^{119}Sn nucleus during the lifetime of the excited state for part of the Sb atoms. We refer to [16,18] for a discussion of this exciting phenomenon. Here we will only use the fact that the Sb atoms associated with the components I_I and I_H are in different environments.

The substrates were n-type float-zone Si wafers with 3 kΩ cm resistivity. Various doses of stable ^{121}Sb were implanted at room temperature with energies of 30, 60, 110, and 220 keV in order to make a reasonably homogeneous profile with an average depth of about 120 nm, as measured by Rutherford backscattering spectrometry. The radioactive probe ^{119}Sb was implanted with 110 keV at a very low dose ($< 1 \times 10^{12}$ cm^{-2}). Recovery of radiation damage was achieved by annealing at 900 °C for 30 min in flowing N_2. This procedure leads to almost 100% substitutional Sb [16].

Hydrogen was introduced by implantation with a typical current of 200 nA cm^{-2} at an energy of 200 eV of
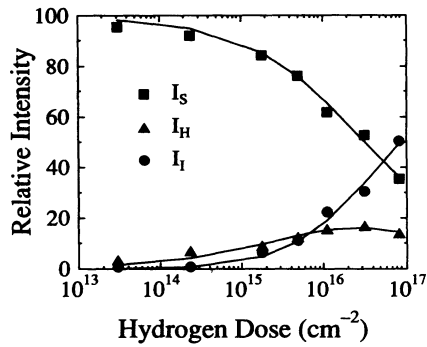
FIG. 1. Relative intensities of the three components as a function of H dose for a sample with an Sb dose of 1×10^{14} cm^{-2}. The H implantation was performed at room temperature. I_S denotes the substitutional fraction; I_H and I_I stand for fractions of Sb atoms associated with one and two H atoms, respectively. The solid lines are fits according to the model.

H_2^+ (100 eV per H atom), which is insufficient to create Frenkel pairs [19]. In order to avoid problems from changing surface conditions, the H-dose dependence of the formation of Sb-H complexes was studied by taking Mössbauer spectra *in situ* in the ultrahigh vacuum ($< 10^{-9}$ mbar) implantation setup. The study of the temperature dependence of the H implantation was done by implanting H at a sample temperature of 110–400 K with a dose of 1×10^{15} cm^{-2}. The stability of the Sb-H complexes was investigated by subsequently annealing the sample for 15 min at stepwise increasing temperatures ranging from 373 to 573 K.

CEMS measurements were performed while the sample was kept at 80 K, with a single-line absorber containing 0.6 mgcm^{-2} Ca^{119}SnO$_3$ in a parallel-plate gas-avalanche type detector [20] moving at room temperature on a standard constant-acceleration drive.

Figure 1 displays the relative intensities of the three components as a function of H dose for a sample that has been implanted with an Sb dose of 1×10^{14} cm^{-2}. Hydrogen was implanted at room temperature. At low H dose I_H appears prior to I_I. However, at high H dose, while I_H seems to saturate, I_I clearly continues to increase as a function of H dose. Furthermore, even at an H dose of nearly 1×10^{17} cm^{-2} there are still 35% of the Sb atoms belonging to the substitutional component. For lower doses of Sb-implanted samples (5×10^{12} and 5×10^{13} cm^{-2}) we observed similar effects [16,18].

Figure 2 shows the relative intensity of the various components as a function of the temperature at which a dose of 1×10^{15} cm^{-2} of hydrogen was implanted. We find that the Sb atoms associate with H already at 110 K. The percentages of Sb atoms that trap hydrogen increase as a function of temperature up to 350 K. At 400 K, I_I suddenly decreases, yet I_H stays the same as at 350 K.

The annealing behavior of these three components is shown in Fig. 3 for a sample implanted at room temperature with Sb dose of 1.5×10^{13} cm^{-2} and H dose of 2×10^{15} cm^{-2}. It is clearly demonstrated that I_I de-
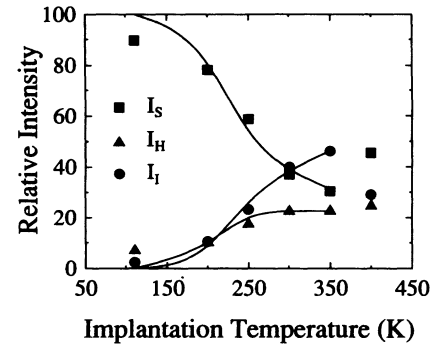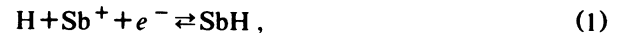

FIG. 2. Relative intensities of the three components as a function of implantation temperature for a sample with an Sb dose of 1.5×10^{13} cm^{-2}. The H dose was 1×10^{15} cm^{-2} for each implantation. The solid lines are fits to the model.

creases at lower temperature than I_H. I_I is shown to decrease at 400 K, while I_H is not changed. This is similar to the observation in Fig. 2 where at 400 K I_I drops down. A complete recovery of I_S is achieved at about 500 K, indicating that all Sb-H complexes have disappeared.

From Fig. 1 we see that I_H appears prior to I_I, suggesting that I_H is an intermediate step for I_I. Moreover, the dose of H is much higher than that of Sb, indicating that there must be other trapping centers for H. In order to understand this behavior quantitatively, we assume that the following reactions take place during hydrogen implantation:

$$H + Sb^+ + e^- \rightleftharpoons SbH , \qquad (1)$$

$$H + SbH \rightleftharpoons SbH_2 , \qquad (2)$$

$$H + H \rightleftharpoons H_2^* , \qquad (3)$$

with the corresponding equilibrium constants

$$k_1(T) = k_{10}\exp(\Delta H_1/kT) = [SbH]/n[Sb^+][H] , \qquad (4)$$

$$k_2(T) = k_{20}\exp(\Delta H_2/kT) = [SbH_2]/[SbH][H] , \qquad (5)$$

$$k_3(T) = k_{30}\exp(\Delta H_3/kT) = [H_2^*]/[H]^2 , \qquad (6)$$
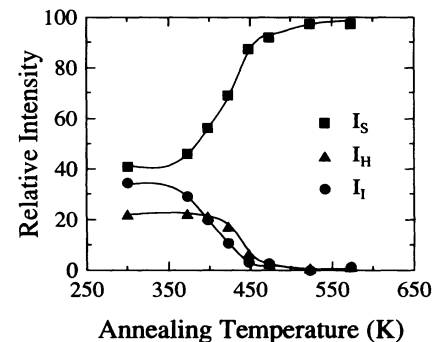

FIG. 3. Relative intensities of the three components as a function of annealing temperature for a sample implanted with an Sb dose of 1.5×10^{13} cm^{-2} and a hydrogen dose of 2×10^{15} cm^{-2}. The implantations were done at room temperature. Solid lines are fits according to the model.

where the brackets indicate the atomic concentrations of the various species; k_{i0} ($i = 1,2,3$) are constants and ΔH_i (> 0) the corresponding binding enthalpies. Furthermore, n is the conduction electron concentration, which is equal to [Sb$^+$] if there are no other donors or acceptors (we will assume $n =$ [Sb$^+$] for the rest of the analysis). For the samples under investigation, the ratio [Sb$^+$]/[Sb^0] can be calculated for different temperatures [21] and we find that [Sb$^+$] $\gg$ [Sb^0]. It is considered that all the products are neutral unless specified otherwise.

In writing down these equations, we have assumed that the concentrations of negatively and positively charged H in our samples are small [6,11]. We will further make the following assumptions: (i) H$_2$* is the main form of hydrogen in the sample; (ii) most of the hydrogen is homogeneously distributed in a range L_H with an average concentration [H]^{tot} = H$_D/L_H$, where H$_D$ is the total hydrogen dose; (iii) thermal equilibrium is achieved for all species at the hydrogen implantation temperature.

With assumption (i) and Eq. (6) the total concentration of hydrogen, [H]^{tot}, can be expressed as follows:

$$[H]^{tot} = 2[H_2{}^*] = 2k_3(T)[H]^2. \tag{7}$$

Furthermore, assumption (ii) and Eq. (7) lead to expressions for [SbH] and [SbH$_2$] as a function of H$_D$:

$$[SbH] = (H_D/2L_H)^{1/2}[Sb^+]^2 k_1(T)/\sqrt{k_3(T)}, \tag{8}$$

$$[SbH_2] = (H_D/2L_H)[Sb^+]^2 k_1(T)k_2(T)/k_3(T). \tag{9}$$

To make use of the model to fit the experimental data, we have to relate the Mössbauer components with the Sb-associated complexes. In our Mössbauer spectra we observe the transition in ^{119}Sn after the decay of the parent ^{119}Sb. We always obtain the same line for the substitutional site, irrespective of the Sb charge state. Therefore, we can write for the substitutional fraction $I_S = c([Sb^+] + [Sb])$, with c a calibration constant. Furthermore, we assume $I_H = c[SbH]$ and $I_I = c[SbH_2]$, so $I_0 = c[Sb]^{tot}$, [Sb]^{tot} being the total Sb concentration.

With respect to the dose dependence, good fits have been achieved as shown with the solid lines in Fig. 1. We also tried to fit the data with other models, for example with [H]^{tot} proportional to [H]. However, these attempts failed. The observed data can be explained only if [H]^{tot} is proportional to [H$_2$*].

Our data on the temperature dependence of the hydrogen implantation can be understood on the basis of the same model. The solid lines in Fig. 2 are fits to the data with the differences in binding enthalpies of the various species as adjustable parameters. We find $\Delta H_1 - \frac{1}{2}\Delta H_3 = -0.073$ eV and $\Delta H_2 - \frac{1}{2}\Delta H_3 = -0.034$ eV, which represent the binding enthalpies of the following equilibria, respectively: $\frac{1}{2}H_2{}^* + Sb^+ + e^- \rightleftarrows SbH$ and $\frac{1}{2}H_2{}^* + SbH \rightleftarrows SbH_2$. The differences in binding enthalpies are negative, indicating that it costs energy for the above reactions going from left to right. Therefore, H$_2$* is the most stable species.

To understand the annealing behavior, we introduce a new parameter $K(T)$, *the rate of disappearance of H from the Sb region*. Based on assumption (i) where [H]^{tot} can be approximated to be 2[H$_2$*], we have

$$\partial[H_2{}^*]/\partial t = -[H_2{}^*]K(T). \tag{10}$$

Using this equation the changes of the Mössbauer components upon annealing can be derived. We find that the annealing processes of all components can be described by a single parameter $K(T)$. The least-squares fitted result is shown with solid lines in Fig. 3. Fits obtained for samples implanted with different doses of Sb and H yield $K(T)$ values that differ at most 20%. The temperature dependence of $K(T)$ corresponds to an activation energy of about 0.2 eV.

We conclude that on the basis of a simple model all three sets of experimental data can be explained. An essential ingredient of this model is the multiple trapping of H in n-type c-Si. From the strikingly good fits of the dose dependence we confirm the assignment that I_H is the Mössbauer component associated with an SbH complex [15,16], whereas the invisible component I_I is assigned to a complex consisting of an Sb and two hydrogen atoms. As we cannot observe the SbH$_2$ fraction directly, we cannot exclude that other species contribute to the invisible fraction, for instance, complexes of the type SbH$_n$, $n > 2$. Such additional complexes, if present, are considered to be part of the SbH$_2$ reservoir.

Questions can be raised concerning the assumptions. The fact that attempts failed to fit the data with a model in which the majority of the hydrogen atoms are present in a form other than H$_2$* strongly suggests that H$_2$* is the dominant form of H in the sample, which justifies assumption (i). Assumption (ii) is reasonable because of the fact that good fits have been obtained using Eqs. (8) and (9), in which the fitting parameters containing L_H turn out to be H-dose independent. The essential assumption (iii) is justified because it provides a correct description of the temperature dependence of the various components and of their annealing behavior.

The fact that the differences in binding enthalpies are small implies that differences in the stability of H atoms in the three forms, i.e., SbH, SbH$_2$, and H$_2$*, are very small. This suggests that the chemical bonding of the H atom in the three forms cannot be very different and involves in all cases a covalent Si-H bond. This is consistent with the models proposed for SbH [3,4], for SbH$_2$ [12,13], and for H$_2$* [8,9,22].

The differences in binding enthalpies are small but significant, because only on this basis can we understand the results on the temperature dependence of the H implantation. These differences in binding enthalpies reflect the enthalpy differences when *an individual hydrogen* is incorporated into different complexes. The results show that an individual hydrogen is bonded most strongly as an H$_2$* complex, which suggests that the majority of H atoms would like to form such a complex, again providing

support for assumption (i). The increase in the intensity of the Sb-H complexes (I_H and I_I) with increasing implantation temperatures can be understood as follows: When the temperature increases the small decrease of the equilibrium concentration of H_2^* in Eq. (3) gives rise to a noticeable increase of the concentration of atomic H, which leads to shifts of the two equilibria in Eqs. (1) and (2) to the right; i.e., we have more Sb-H complexes.

The data in Fig. 2 for 110 K deviate from the theoretical curves. The model predicts that no Sb-H complexes form at 110 K, but small percentages of I_H and I_I do appear, as shown in Fig. 2. This deviation may be due to the violation of assumption (iii); i.e., no equilibrium is established at this temperature. When a H atom is trapped by an Sb atom, it will stay there. However, the formation of SbH_2 requires an intermediate state (SbH) and therefore I_I is nearly zero. Also the model cannot fit the data at 400 K, where I_I decreases dramatically. This is due to the failure of assumption (ii); i.e., $[H]^{tot}$ is no longer proportional to the H dose (H_D), because at this temperature H starts to diffuse out of the Sb region.

We remark that I_I anneals out at a slightly lower temperature than I_H, *but this does not necessarily mean that SbH_2 has a smaller dissociation energy.* The annealing behavior of the three Mössbauer components can be described well by the single parameter $K(T)$. Therefore, the determining step in the dissociation is the sudden reduction of the H_2^* concentration because this species is able to escape from the Sb donor region. This view is supported by SIMS data on hydrogen profiles (Fig. 1 of Ref. [7]), from which we find that the concentration of $^2H_2^*$ in the surface region (< 0.5 μm) decreases in the same temperature region as our Sb-H complexes do (Fig. 3). The apparent difference in dissociation temperatures for SbH and SbH_2 shown in Fig. 3 is caused by the fact that the production of SbH is an intermediate step during the dissociation of SbH_2. We note that it is not justified to derive the dissociation enthalpies for the SbH complex neglecting recombination, as was done earlier [1,15,16]. Moreover, we expect that an analogous PH_2 complex exists in the samples of Ref. [14]. The formation of PH_2 will possibly lead to passivation. Therefore, the dissociation energy (1.18 eV) of PH derived from the capacitance-voltage measurements [14] should be reinterpreted, because in this case, both PH and PH_2 will affect the depth profiles of the donor concentration.

Summarizing, we have obtained direct information on the Sb-H complexes in n-type c-Si using Mössbauer spectroscopy. Strong evidence has been provided for multiple trapping of H. Also the differences in binding enthalpies for the three H complexes are obtained from the model fit to the Mössbauer data. The small differences in binding enthalpies provide experimental support for the theoreti-

cal models proposed for the H complexes. Furthermore, it is shown that the annealing behavior of the different H complexes is governed by the rate at which H_2^* is able to escape from the dopant region.

[1] K. Bergman, M. Stavola, S. J. Pearton, and J. Lopata, Phys. Rev. B 37, 2770 (1988).

[2] S. M. Myers et al., Rev. Mod. Phys. 64, 559 (1992).

[3] P. J. H. Denteneer, C. G. Van de Walle, and S. T. Pantelides, Phys. Rev. B 41, 3885 (1990).

[4] S. B. Zhang and D. J. Chadi, Phys. Rev. B 41, 3882 (1990).

[5] J. W. Corbett, S. J. Pearton, and M. Stavola, in Defects Control in Semiconductors, edited by K. Sumino (North-Holland, Amsterdam, 1990), p. 53.

[6] C. Herring and N. M. Johnson, in Hydrogen in Semiconductors, edited by J. I. Pankove and N. M. Johnson, Semiconductors and Semimetals Vol. 34 (Academic, New York, 1991), Chap. 10.

[7] N. M. Johnson and C. Herring, Phys. Rev. B 43, 14297 (1991).

[8] K. J. Chang and D. J. Chadi, Phys. Rev. Lett. 62, 937 (1989).

[9] K. J. Chang and D. J. Chadi, Phys. Rev. B 40, 11644 (1989).

[10] N. M. Johnson et al., Mater. Sci. Forum 83-87, 33 (1992).

[11] C. H. Seager, R. A. Anderson, and D. K. Brice, J. Appl. Phys. 68, 3268 (1990).

[12] L. Korpas, J. W. Corbett, and S. K. Estreicher, Mater. Sci. Forum 83-87, 27 (1992).

[13] L. Korpas, J. W. Corbett, and S. K. Estreicher, Phys. Rev. B 46, 12365 (1992).

[14] J. Zhu, N. M. Johnson, and C. Herring, Phys. Rev. B 41, 12354 (1990).

[15] Z. N. Liang and L. Niesen, Hyperfine Interact. 60, 749 (1990).

[16] Z. N. Liang and L. Niesen, Mater. Sci. Forum 83-87, 99 (1992).

[17] N. N. Greenwood and T. C. Gibb, Mössbauer Spectroscopy (Chapman and Hall, London, 1971).

[18] Z. N. Liang and L. Niesen, Nucl. Instrum. Methods. Phys. Res., Sect. B 63, 147 (1992).

[19] G. F. Cerofolini et al., Phys. Rev. B 41, 12607 (1990).

[20] G. Weyer, Mössbauer Effect Methodology 10, 301 (1976).

[21] M. A. Green. J. Appl. Phys. 67, 2944 (1990).

[22] S. B. Zhang and W. B. Jackson, Phys. Rev. B 43, 12142 (1991).